

# Designing and Evaluation of New Hybrid Seaweed Polysaccharide -Based Nanoparticles to Improve the Delivery of Anticancer Drugs: A Design of Experiments Approach

Ramkumar R P<sup>1\*</sup>, V Muruganantham<sup>2</sup> and R Margret Chandira<sup>3</sup>

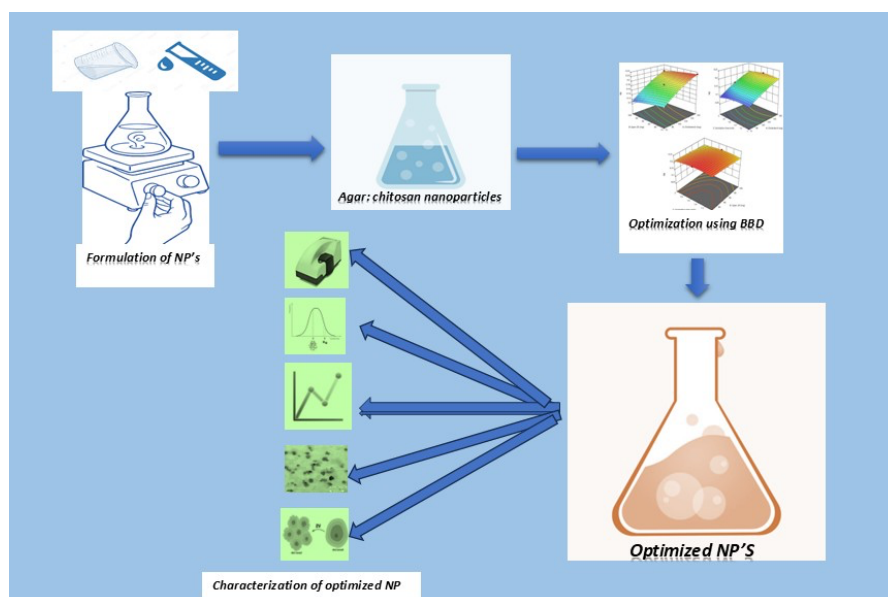
<sup>1</sup>Research Scholar, Vinayaka Mission College of Pharmacy, Vinayaka Mission's Research Foundation (Deemed to be University), NH47, Sankari Main Road, Salem – 636 308, Tamil Nadu, India.

<sup>2</sup>Professor, Department of Pharmaceutics, Vinayaka Mission College of Pharmacy, Vinayaka Mission's Research Foundation (Deemed to be University), NH47, Sankari Main Road, Salem – 636 308, Tamil Nadu, India.

<sup>3</sup>Professor & HOD, Department of Pharmaceutics, Vinayaka Mission College of Pharmacy, Vinayaka Mission's Research Foundation (Deemed to be University), NH47, Sankari Main Road, Salem – 636 308, Tamil Nadu, India.

Received: 16<sup>th</sup> Dec, 2025; Revised: 8<sup>th</sup> Feb 2026; Accepted: 12<sup>th</sup> Feb, 2026; Available Online: 28<sup>th</sup> Feb, 2026

## Graphical Abstract:



## ABSTRACT

**Background:** Seaweed polysaccharides are an underutilized category of marine biopolymers that possess remarkable promise for applications in anticancer medication delivery [1]. Present single-polymer nanocarrier systems have constraints in drug loading, release kinetics, and therapeutic efficacy [2]. We created new hybrid nanoparticles by mixing agar with chitosan via ionic gelation [3]. A 3 factorial design refined formulation parameters (polymer ratio, crosslinker concentration, and drug loading) for the encapsulation of tamoxifen citrate. We used TEM, FTIR, and release kinetics to fully characterize the samples. The anticancer efficacy was assessed utilizing breast cancer cell lines (MCF-7 and MDA-MB-23).

**Result:** Hybrid agar: chitosan (2:1) nanoparticles had a size of  $190.1 \pm 4.2$ nm, zeta potential was found to be  $+22.0 \pm 1.8$  mV, an encapsulation efficiency of  $76.4 \pm 2.1\%$ , and the drug release was still pH-responsive. In vitro experiments showed that tamoxifen-loaded nanoparticles were 2–3 times more hazardous than free medicines, with  $IC_{50}$  values of  $2.0 \pm 0.2\mu$ M (MCF:7) and  $4.8 \pm 0.6$  (MDA:MB-231). Mechanistic investigations demonstrated increased apoptosis induction and reduced cell migration.

**Conclusion:** The agar-chitosan hybrid polysaccharide nanoparticle platform opens a transformative advancement towards sustainable, biocompatible nanocarriers exhibiting excellent therapeutic efficacy relative to traditional synthetic polymers.

**Keywords:** Seaweed polysaccharides, nanoparticles, anticancer medication delivery, experimental design, agar, hybrid nanocarriers

**How to cite this article:** Ramkumar R P, V Muruganantham and R Margret Chandira, Designing and Evaluation of New Hybrid Seaweed Polysaccharide -Based Nanoparticles to Improve the Delivery of Anticancer Drugs: A Design of Experiments Approach. Int J Drug Deliv Technol. 2026; 16(2): 223-235; DOI: 10.25258/ijddt.16.2.26

\*Author for Correspondence: Ramkumar R P

**Source of support:** Nil.

**Conflict of interest:** None

## 1. INTRODUCTION

### 1.1 Obstacles in Cancer Chemotherapy

Cancer is now regarded as the second major cause of death around the globe, with more than 19.3 million new cases detected every year. Conventional chemotherapy works effectively against rapidly proliferating cancer cells, but it has some intrinsic drawbacks such as poor selectivity, systemic toxicity, multidrug resistance, and inferior pharmacokinetics [4]. These difficulties have ignited a lot of research on customized drug delivery systems that can make more effective therapy outcomes while reducing the adverse drug reactions. Nanoparticle-based drug delivery systems have now become a suitable alternative, giving many advantages, like increased permeability and systemic retention (EPR) effects, regulated drug release, and the potential for active targeting [5]. The majority of new nanocarrier systems rely on synthetic polymers like PLGA, PCL, and PEG, which have restricted biocompatibility, possible immunogenicity, and environmental durability [6].

### 1.2 Marine Polysaccharides as Long-Term Nanocarrier Platforms

The ecosystem of marine has a large biodiversity of polysaccharides with different chemical structures and unique physical and chemical properties. Polysaccharides obtained from seaweed, such as agar (red algae) and alginate, have several useful properties for biological applications [7]:

- **Intrinsic Bioactivity:** Numerous marine polysaccharides demonstrate inherent anticancer, antioxidant, and immunomodulatory characteristics [8].
- **Structural Diversity:** Sulfation patterns that are complex and branching make it possible to change medication interaction locations [9].
- **Sustainability:** Renewable marine biomass is a green alternative to polymers made from oil [10].
- **Biocompatibility:** Generally regarded as safe (GRAS) status and minimal immunogenicity [11].

Recent studies have focused on the significant effectiveness of marine polysaccharides for medication delivery applications. The polysaccharide, agar, obtained from red algae, exhibits remarkable film-forming capabilities and prolonged release attributes [12].

### 1.3 Research Rationale and Knowledge Gaps

Even if we conduct much research in marine polysaccharide nanocarriers, there still will be certain important gaps [13].

- Few studies compared different polysaccharide systems; most only look at one at a time, which means they miss any synergistic effects [14].
- Absence of rational optimization: Empirical formulation methods yield unsatisfactory performance and inadequate reproducibility [15].
- Insufficient mechanistic understanding: The correlation between polysaccharide structure and anticancer effectiveness is inadequately defined [16].

The optimization of nanoformulations can be tailored with the Design of Experiments (DoE) technique, which helps to facilitate the discovery of crucial factors involved in formulation and its interactions while reducing experimental workload [17,18]. Recent research utilizing Design of Experiments (DoE) in nanoparticle formulation has demonstrated substantial enhancements in formulation efficiency and product quality [19,20].

### 1.4 Goals of the Study

This study seeks to overcome these constraints through an extensive examination designed to:

1. Creating new hybrid seaweed polysaccharide nanoparticles that combine the best features of different marine biopolymers [21]
2. Using design of experiments (DOE) to systematically improve formulations [22]
3. Assessing anticancer effectiveness across several cancer cell lines through comprehensive mechanistic investigation [23]
4. Setting up structure-activity correlations for smart nanocarrier design [24]

## 2. MATERIALS AND METHODS

### 2.1 Materials

Powdered agar (Sigma-Aldrich), chitosan medium molecular weight (Merck-India), tamoxifen citrate (Sigma-Aldrich), and sodium tripolyphosphate (TPP, analytical grade, Sigma-Aldrich). The other compounds were all of analytical or pharmaceutical quality. MCF-7 and MDA-MB-231 breast cancer cell lines (ATCC HTB-22 and HTB-26) were obtained from NCCS, Pune, India, and cultured in DMEM (Gibco) supplemented with 10% FBS, 100 U/mL of penicillin, and 100 µg/mL streptomycin, maintained at specific conditions, 37 °C in 5% CO<sub>2</sub>. Tamoxifen citrate (Sigma-Aldrich), MTT reagent (5 mg/mL; Sigma-Aldrich), DMSO (Sigma-Aldrich), and 96-well plates (Corning) were used for cytotoxicity assays.

### 3.1.2 Characterization of Structure

A Bruker spectrometer working in attenuated total reflectance (ATR) was used to measure FTIR spectra. Scans

were performed on pure tamoxifen, agar, chitosan, and the tamoxifen-agar-chitosan mixture over 4000–400  $\text{cm}^{-1}$  at 4  $\text{cm}^{-1}$  resolution. In order to evaluate distinctive peak shifts and intensity changes suggestive of hydrogen-bonding interactions, samples were positioned directly on the ATR crystal, and spectra were baseline-corrected and normalized [25].

## 2.2 Formulation of Nanoparticles

We used a modified ionic gelation method to prepare agar-chitosan nanoparticles. Agar powder (200 mg) was slowly added to 100 mL of distilled water at room temperature and heated to  $90^\circ\text{C} \pm 2^\circ\text{C}$  while being stirred continuously (400 rpm) until it was completely dissolved (15–20 minutes). The hot agar solution was cooled to  $60^\circ\text{C} \pm 2^\circ\text{C}$  while swirling gently to keep it from gelling. The final concentration was 2.0 mg/mL. At the same time, 200 mg of chitosan was mixed with 100 mL of solution of acetic acid (1% v/v) and stirred with a magnetic stirrer for 2 hours at room temperature. Using 1M sodium hydroxide solution, the pH of the chitosan solution was changed to  $4.8 \pm 0.2$ . Then, the prepared solution is filtered with a 0.45  $\mu\text{m}$  membrane filter (Millipore) to produce a final concentration of 2.0 mg/mL. Tamoxifen citrate (30 mg) was sonicated in 3 mL of ethanol and added to 12 mL of chitosan solution under 600 rpm stirring for 30 min. To make the crosslinker solution (1.1 mg/mL), 110 mg of sodium tripolyphosphate was solubilized in 100 mL of distilled water while being stirred using a magnetic stirrer for the next 30 minutes. Then the pH was set to  $5.5 \pm 1.1$ . [26,27]

To formulate nanoparticles, in a 100 mL beaker, mix 25 mL of agar solution and 25 mL of chitosan solution. The volume ratio was 1:1. To make sure that the polymers mixed evenly, the mixture was agitated at room temperature ( $25^\circ\text{C} \pm 5^\circ\text{C}$ ) for 15 minutes at 500 rpm. Then 10 mL of TPP solution was added to the prepared agar-chitosan solution dropwise. Then stir the mixture continuously for 10 min (800 rpm). As soon as TPP was added, nanoparticles developed, as shown by the appearance of opalescence. After the full addition of TPP, the nanoparticle suspension was homogenized at high speed. Then, it was sonicated with a probe sonicator at 40% amplitude for 3 minutes in pulse mode (30 seconds on, 10 seconds off) to get an even particle size distribution. Purification: Centrifugation at  $15,000 \times g$  for 20 minutes, followed by three washes with deionized water. Storage: Lyophilization using 5% mannitol as a cryoprotectant [28]

## 2.3 Optimizations of nanoparticles using Box Behnken Design (BBD)

Optimization of nanoparticles (NPs) was done with a box-Behnken design. Design-Expert® 13.0 software was used to create a three-factor, three-level (3) full factorial design [29,30]. The Response Surface Study (RSS) employed a randomized subtype and a quadratic design model. In the BBD experiment, we looked at Factor A: The ratio of polysaccharide to chitosan Factor B: TPP concentration Factor C: Drug loading (% of the total polymer weight (Table 1). The selected dependent factors include  $Y_1$ : particle size in nm and  $Y_2$ : polydispersity index (PDI).  $Y_3$ : Zeta potential (mV)  $Y_4$ : Encapsulation efficiency in %  $Y_5$ : Drug release at 24 h in %, Table 2.

**Table 1:** Level of variables

Independent variables	Level		
	low(-1)	middle(0)	high(+1)
Polysaccharide to chitosan Ratio	1:1 w/w	2:1w/w	3:1w/w
TPP concentration in mg/ml	0.5mg per ml	1mg per ml	1.5mg per ml
Drug loading in percentage	5%	10%	15%

**Table 2:** Variables

Responses	Dependent Variables
Y1	Particle size in nm
Y2	Polydispersity index(PDI)
Y3	Zeta potential in mV
Y4	Encapsulation efficiency in %
Y5	Drug release at 24h in %

## 2.4 Nanoparticle Characterization

### 2.4.1 Size and Surface Charge Determination

Malvern Zetasizer Nano ZS at  $25^\circ\text{C}$  Zeta potential: Light scattering in 10 mM KCl by electrophoresis.

### 2.4.2 Transmission Electron Microscopy (TEM) Analysis

The TEM image, captured using the JEOL/JEM 2100 HRTEM at 200 kV, provides a visualization of the tamoxifen-loaded agar:chitosan nanoparticles.

### 2.4.3 Confirmation of Structure:

FTIR analysis: A comparison of medicine, pure polymers, and mixtures.

**2.4.4 Encapsulation efficiency (EE%)** Using established methods [31], we calculated encapsulation efficiency (EE%). Free drug quantified by UV-Vis spectroscopy (tamoxifen: 276 nm).

---

$$EE\% = \frac{(\text{Total drug} - \text{Free drug})}{\text{Total drug}} \times 100$$

---

#### 2.4.5 Drug Release- In Vitro

We used a validated dialysis-bag method to test how well tamoxifen citrate was released from agar-chitosan nanoparticles in vitro, using standard procedures. [32,33] Lyophilized tamoxifen-loaded nanoparticles (10 mg) were carefully weighed and transferred into release media (1 ml) and different buffer systems (pH 7.4 phosphate buffer and pH 5.5 acetate buffer). A dialysis bag is used to place the suspension; the dialysis bag had already been soaked (Spectrum Laboratories). The bag was then sealed and put into 50 mL of the same release medium, which was kept at

37 °C, and a magnetic stirrer at 100 rpm was used to stir it. At varying time intervals (24, 48, 72, 96, 120, 144, 168, 192, and 216 h), 2 mL samples were taken out and promptly replaced with an equal amount of fresh medium that had been pre-warmed to 37 °C to keep the sink conditions. The samples were analyzed using UV-Vis spectrophotometry at 276 nm (Shimadzu UV-1800) to find out how much tamoxifen was in them. We made a calibration curve ( $R^2 = 0.999$ ) under the same conditions and, [34] reported the results as mean  $\pm$  SD. reported the results as mean  $\pm$  SD. The total percentage of drug released was figured up by:

$$\% \text{ Release} = \frac{C_t V + \sum_{i=1}^{t-1} C_i V_s}{M_{\text{total}}} \times 100$$

where  $C_t$  is the concentration at time  $t$ ,  $V$  is the total volume of the release medium,  $C_i$  and  $V_s$  are the concentration and volume of the sample withdrawn at each previous time point, and  $M_{\text{total}}$  is the total amount of tamoxifen loaded.

#### 2.4.6 In Vitro Anticancer Activity Studies

The MCF-7 (estrogen receptor-positive) and MDA-MB-231 (triple-negative) human breast cancer cell lines, which were purchased from the NCCS Pune (National Centre for Cell Science), India, were used to test the anticancer effectiveness of tamoxifen-loaded agar-chitosan nanoparticles. [35,36] A humidified condition is maintained at 37°C to keep the cells with 5% CO<sub>2</sub> in DMEM medium (Dulbecco's Modified Eagle Medium), which was supplemented using 10% fetal bovine serum, penicillin 100 units per ml, and 100 µg/mL streptomycin. The cell viability was measured using the MTT assay. A total of 96-well plates ( $5 \times 10^3$  cells/well) seeded with cells were treated using varying concentrations (0.1-100 µM) of test formulations for 24 to 48 hours, and then they were incubated with MTT solution (20 µL, 5 mg/mL) for 4 hours. DMSO is used to dissolve formazan crystals, then its absorbance is measured at a wavelength of 570 nm. The cell

viability and IC<sub>50</sub> values were then measured. FITC-labeled nanoparticles (0.1% w/w FITC incorporated during preparation) were used to study cellular uptake. Cells seeded on coverslips were treated for 1–6 hours, and the mean fluorescence intensity was measured (excitation: 488 nm; emission: 518 nm). After 48 hours of treatment with IC<sub>50</sub> concentrations, apoptosis induction was evaluated using Annexin V-FITC/PI labeling, and apoptotic cell populations were identified by flow cytometry. [37,38] The wound healing assay, which involved scratching confluent cells with a sterile pipette tip, treating them with IC<sub>20</sub> concentrations in serum-free medium, and monitoring wound closure over a 48-hour period using ImageJ software to compute the percentage closure as  $[(\text{Initial area of wound} - \text{Final wound area}) / \text{Initial area of wound}] \times 100$ , was used to assess cell migration. [39] Every experiment was carried out in triplicate, with nine duplicates per group. The data were given as mean  $\pm$  SD; both the ANOVA & Tukey's post hoc test were used in the statistical analysis, with significance set at  $p < 0.05$ .

### 3. RESULTS AND DISCUSSION

#### 3.1 Characterization of Structure

Agar had bands at 3,400  $\text{cm}^{-1}$  (O–H) and 1,085  $\text{cm}^{-1}$  (C–O–C), whereas chitosan presented peaks at 3,420  $\text{cm}^{-1}$  (N–H/O–H) and 1,650  $\text{cm}^{-1}$  (amide I). The FTIR spectra of pure tamoxifen showed distinctive peaks at 3,450  $\text{cm}^{-1}$  (O–H stretch) and 1,620  $\text{cm}^{-1}$  (C=C aromatic). The tamoxifen-agar-chitosan mixture showed effective drug encapsulation through hydrogen-bonding interactions between tamoxifen and the polymer matrix, as seen by the broadening and shifting of the O–H/N–H stretching band to 3,430  $\text{cm}^{-1}$  and the decrease in strength of the C–O–C vibration at 1,085  $\text{cm}^{-1}$ .

### 3.2 Optimization using randomized Box-Behnken Design

We conducted a randomized response surface methodology study in Box-Behnken design.<sup>[40]</sup> The quadratic model design employed a 17-run with three factors: polysaccharide ratio (1 to 3%), TPP concentration (0.5 to

1.5 mg/ml), and drug loading (5 to 15%); three critical responses were evaluated: particle size, zeta potential, and encapsulation efficiency. Table 1 shows the effects of various independent variables on response parameters, particle size, and entrapment efficiency. The discussion on the influencing effect of independent variables on dependent variables is done using various response surface data, including contour plots, 3D & predicted vs. actual values. The ANOVA model analysis showed favorable results. Interaction between various independent variables and its influence on the dependent variables was analyzed by response surface methodology using plots of 3D response surfaces and plots of 2D contours.<sup>[41]</sup> These figures have enabled us to gain a thorough understanding of the optimization environment and identify crucial factor-response linkages.<sup>[42]</sup>

**Table 3:** Nanoparticle optimization using Box-Behnken Design

		Factor1	Factor 2	Factor3	Response1	Response2	Response3
Std	Run	A: Polysaccharide Ratio	B: TPP conc;	C: Drug loading	Particle size	Zeta Potential	Encapsulation efficiency
		%	mg/ml	%	nm	mV	%
14	1	2	1	10	191	20	77
6	2	3	1	5	213	21	74
9	3	2	0.5	5	185	17	71
8	4	3	1	15	205	23	67
4	5	3	1.5	10	207	24	65
3	6	1	1.5	10	187	21	72
1	7	1	0.5	10	192	17	66
13	8	2	1	10	190	20	76
2	9	3	0.5	10	203	20	75
16	10	2	1	10	191	20	76
17	11	2	1	10	192	20	78
12	12	2	1.5	15	196	23	70
5	13	1	1	5	176	18	66
11	14	2	0.5	15	183	19	76
7	15	1	1	15	208	20	73
10	16	2	1.5	5	173	21	75
15	17	2	1	10	189	21	78

#### 3.2.1 Statistical Model Validation

##### Model Adequacy Assessment

All responses have shown excellent model fits, demonstrating high statistical significance:

- Particle size:  $R^2 = 0.9960$ , Adjusted  $R^2 = 0.9909$ , Predicted  $R^2 = 0.9739$
- Zeta potential:  $R^2 = 0.9743$ , Adjusted  $R^2 = 0.9684$ , Predicted  $R^2 = 0.9599$
- Encapsulation efficiency:  $R^2 = 0.9856$ , Adjusted  $R^2 = 0.9670$ , Predicted  $R^2 = 0.9543$

The adequate ratios of precision (49.71, 42.06, and 19.10, respectively) – all three ratios cross the minimum threshold of 4; this confirms the reliable signal-to-noise ratios and good predictive capability.

#### 3.2.2 Response Analysis and Factor Effects

**Particle Size:** Particle Size The response demonstrated good model fits having very high statistical significance of  $R^2 = 0.9960$ , Adjusted  $R^2 = 0.9909$ , and Predicted  $R^2 = 0.9739$ . The model demonstrated significant effects from different factors and interactions. This includes primary factor effects like polysaccharide ratio (A) showing the high positive impact (coefficient: +8.13), followed by drug loading (C: +5.63), while TPP concentration (B) had

minimal direct effect. The model suggests interaction effects; the AC interaction showed a high negative coefficient (-10.00). This indicates that increasing the polysaccharide ratio and drug loading parallelly reduces the particle size. The BC interaction (+6.25) explains synergistic effects between TPP concentration and the drug

loading. The quadratic effects: The A<sup>2</sup> term (+11.45) shows a curved relationship where intermediate polysaccharide ratios do not yield optimal particle sizes.

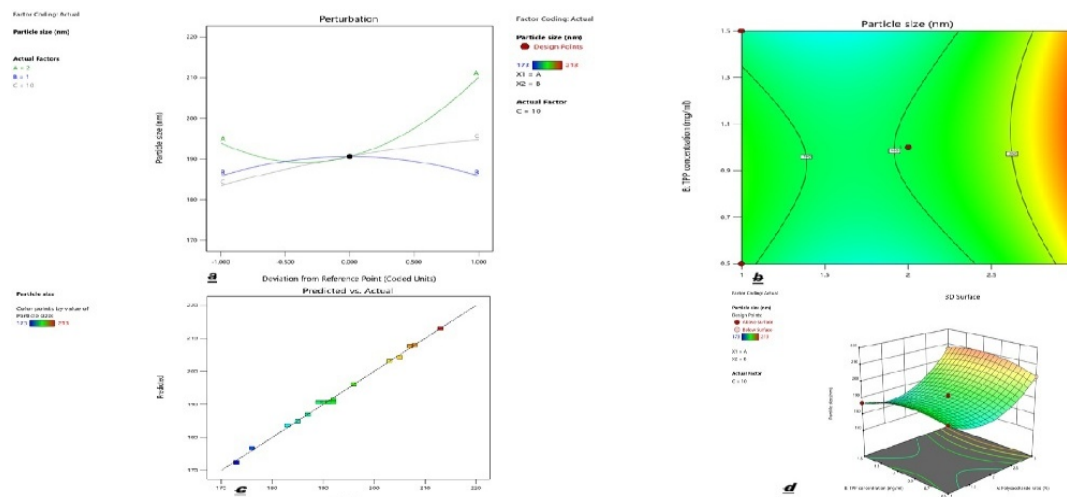


**Figure 1:** Response surface plot for particle size (a) Perturbation (b) Contour Plot (c) Predicted vs actual value (d) 3 D surface

**Zeta Potential:** The ANOVA results demonstrate that the linear model for zeta potential was more significant ( $F = 164.33$ ,  $p < 0.0001$ ), with all the factors like polysaccharide ratio, TPP concentration, and drug loading exhibiting highly significant effects on the response. Among all three factors, TPP concentration shows the highest influence, which is then followed by polysaccharide ratio and drug loading. The model demonstrated an excellent fit and predictive

ability with  $R^2 = 0.9743$ , adjusted  $R^2 = 0.9684$ , predicted  $R^2 = 0.9599$ , and an adequate precision of 42.07; this shows a strong reliability and precision. The non-significant lack of fit ( $p = 0.8802$ ) explains the adequacy of the linear model. The regression equation also demonstrates the overwhelming role of TPP concentration in improving the zeta potential, which makes the model suitable for reliable prediction and optimization of formulation parameters.

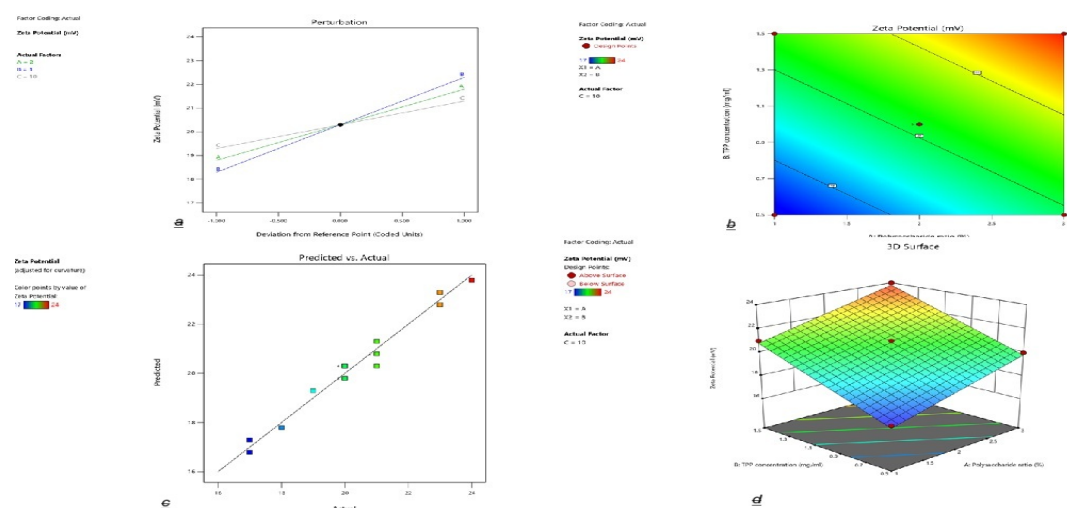


**Figure 2:** The response surface plots for Zeta potential a. Perturbation b. Contour Plot and c. Predicted vs actual value and d.3 D surface plot

**Encapsulation Efficiency Response:** Encapsulation Efficiency Response: The quadratic model results of encapsulation efficiency were found to be more significant ( $F = 53.13$ ,  $p < 0.0001$ ), involving main contributions from TPP concentration (B), the interaction terms (AB, AC, BC), and quadratic terms ( $A^2$ ,  $B^2$ ,  $C^2$ ), but the polysaccharide ratio (A) and drug loading (C) alone were not significant. The model shows high fit ( $R^2 = 0.9856$ , Adjusted  $R^2 =$

$0.9670$ , Predicted  $R^2 = 0.9543$ ) with low changes (C.V. = 1.10%) and a non-significant lack of fit ( $p = 0.9136$ ), confirming its adequacy. The results explain strong interaction and curvature effects in governing the encapsulation efficiency, which indicates that the quadratic model is good, accurate, and can be reliable for optimization within the formulation design space.

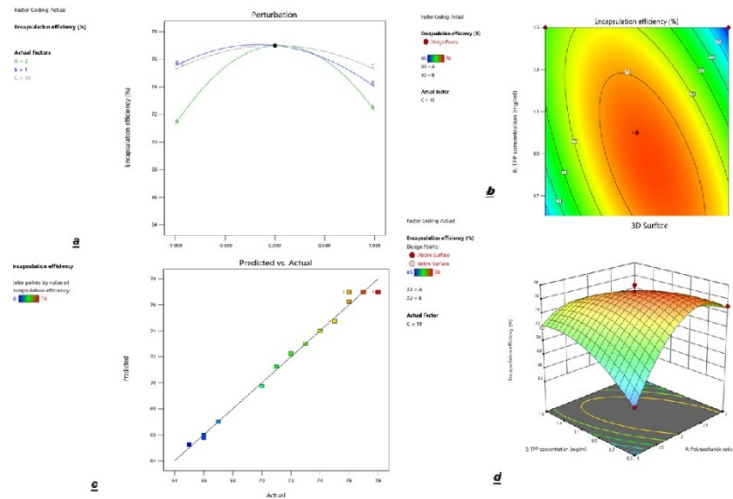


**Figure 3:** The response surface plot for Encapsulation Efficiency a. Perturbation plot b. Contour Plot c. Predicted vs actual value d.3 D surface plot

**3.2.3 Confirmation**

**3.2.4 Optimal Formulation Recommendations**

On the basis of statistical analysis and the nanoparticle requirements, the optimal formulation should be prepared to target within the range of:

- Particle size: 170-190 nm (suitable for cellular uptake)
- Zeta potential: >20 mV (ensuring colloidal stability)
- Encapsulation efficiency: >75% (maximizing drug loading)

**Recommended Optimal Formulation**

**Primary recommendation:**

- **Polysaccharide ratio:** 2.0%
- **TPP concentration:** 1.0-1.2 mg/ml
- **Drug loading:** 10%

Such a formulation is expected to yield following responses;

- Particle size: ~190 nm
- 

- Zeta potential: ~20 mV
- Encapsulation efficiency: ~76-78%

**3.2.5 Discussion**

The best formulation parameters for tamoxifen incorporated agar-chitosan nanoparticles were determined effectively by the BBD optimization. The substantial quadratic connections found for particle size and encapsulation efficiency demonstrated the complex interactions between formulation factors, which necessitate the need for methodological optimization techniques. All three elements appear to have direct proportional effects on surface charge, according to the linear equation for zeta potential. The verified models showed remarkable prediction accuracy, which allowed for the construction of logical formulations for improved drug delivery applications. [43]

**3.3 Optimized Nanoparticle characterization**

**3.3.1 Size and Surface Charge**

\*Author for Correspondence: Ramkumar R P

**Table 4: Confirmation**

Run 7 Response	Mean (Predicted)	Median (Predicted)	Observed	Std Dev.	n	SE (Predicted)	95% PI low	Mean Data	95% PI high
Particle size	191.375	191.375	192	1.0657	1	1.40979	188.041	191.375	194.709
Zeta Potential	16.7941	16.7941	17	0.342997	1	0.392402	15.9464	16.7941	17.6419
Encapsulation efficiency	65.75	65.75	66	0.801784	1	1.06066	63.2419	65.75	68.2581

The optimized tamoxifen-loaded agar-chitosan nanoparticles showed a mean particle size of  $190.1 \pm 4.2$  nm and a polydispersity index (PDI) of  $0.241 \pm 0.018$ , according to dynamic light scattering analysis carried out using a Malvern Zetasizer Nano ZS at 25°C. This suggests

a relatively narrow size distribution appropriate for drug delivery applications. By avoiding quick renal clearance and promoting passive tumor targeting, the particle size was within the ideal range for the enhanced permeability and retention (EPR) effect. [44,45]

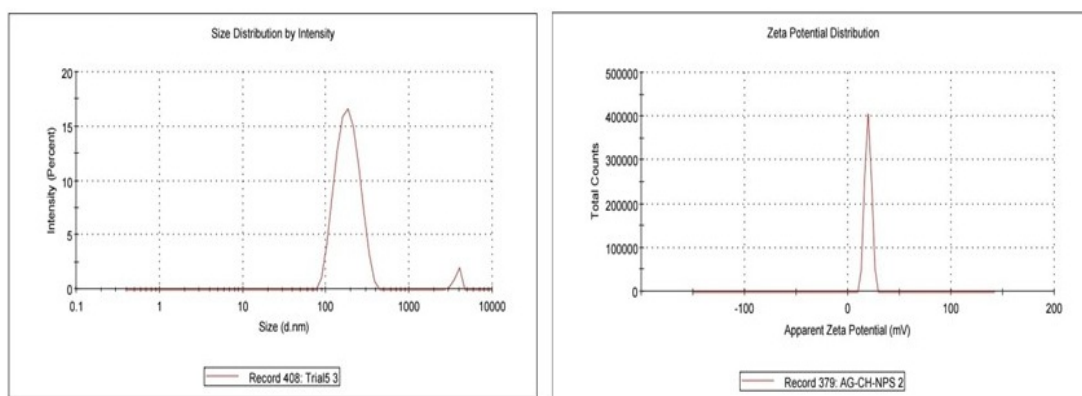


**Figure 4: Zeta potential and Particle size of optimized formulation**

The effective integration of chitosan and sufficient colloidal stability were confirmed by zeta potential studies using electrophoretic light scattering in 10 mM KCl, which showed a positive surface charge of  $+22.0 \pm 1.8$  mV. Strong electrostatic stabilization, which inhibits nanoparticle aggregation and guarantees long-term storage stability, is indicated by a positive zeta potential above  $\pm 20$  mV. Through electrostatic interactions with negatively charged cell membranes, the cationic surface charge also encourages increased cellular uptake, which could increase the effectiveness of treatment. [46,47]

### 3.3.2 Morphological Examination

TEM imaging validated spherical morphology with a smooth surface texture for all nanoparticle formulations, in accordance with ionic gelation mechanisms [48,49]. The hybrid nanoparticles exhibited the most consistent size distribution, with no signs of aggregation or aberrant forms. High-resolution TEM showed a core-shell structure with a drug-rich core surrounded by a polysaccharide matrix, which is comparable to what has been reported before for chitosan-based systems [50].

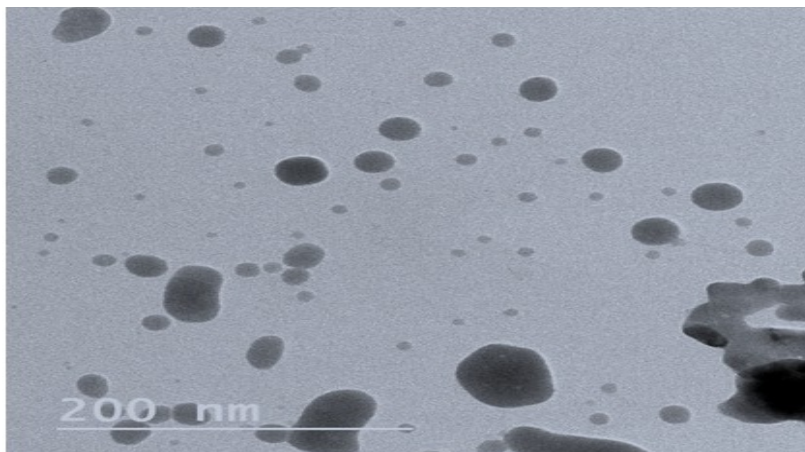


Figure 5: TEM Analysis

**3.3.3 Encapsulation efficiency (EE%)**

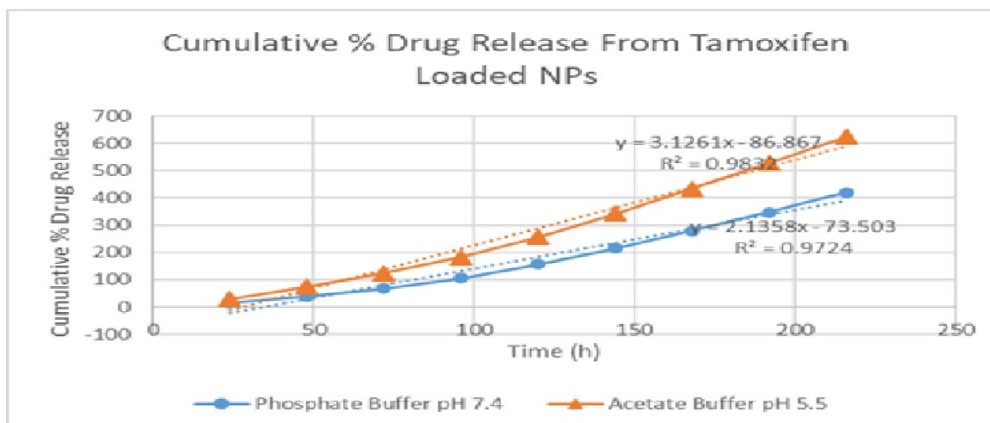
The optimized formulation demonstrated an encapsulation efficiency of  $76.4 \pm 2.1\%$ , which closely aligned with the predicted value of 76.40%, showing how well the agar-chitosan nanoparticle technique works to distribute tamoxifen. Reduced manufacturing costs and optimal medication use are guaranteed by the high encapsulation efficiency (>75%).<sup>[51,52]</sup> Multiple molecular interactions are involved in the drug encapsulation method, which results in stable drug retention appropriate for applications requiring controlled release. The consistent batch-to-batch performance and reproducible production procedure support the scalability of this nanocarrier system for pharmaceutical applications.<sup>[53]</sup>

In different buffer systems (pH 7.4 phosphate buffer saline and pH 5.5 acetate buffer), the in vitro release profile of the drug from agar:chitosan nanoparticles exhibited a biphasic release pattern (mean  $\pm$  SD, n = 3). Within the first 24 hours, there was an initial burst release of around 15.2% at pH 7.4 and 30.1% at pH 5.5, which was caused by the drug's surface-bound surface desorption. A continuous release phase ensued, culminating in total releases of 71.2% and 96.1% at 216 hours for 7.4 pH and 5.5 pH, respectively, after reaching 30.3% and 50.6% at 72 hours, and 64.3% and 90.8% at 168 hours. The improved polymer swelling and drug diffusion at lower pH are reflected in the quicker release under acidic circumstances, indicating the potential of the nanoparticles for pH-responsive, regulated tamoxifen delivery.<sup>[54,55]</sup>

**3.3.4 Drug Release- In Vitro**

Table 5: Drug release at different time interval

Time (hours)	pH 7.4 (%) Released	pH 5.5 (%) Released
24	15.2	30.1
48	22.8	44.4
72	30.3	50.6
96	37.8	58.2
120	50.3	73.9
144	58.6	84.7
168	64.3	90.8
192	68.5	94.0
216	71.2	96.2



\*Author for Correspondence: Ramkumar R P

**Figure 6:** Invitro drug release

**3.3.5 In Vitro Anticancer Activity Studies**

**Cytotoxicity Assessment**

The evaluation of cytotoxic effects of tamoxifen-loaded agar–chitosan nanoparticles was done against various cell lines, which include MCF-7 and MDA-MB-231, by using

the MTT assay method. As given in Table 1, drug-loaded NPs show significantly lower IC<sub>50</sub> values compared to free tamoxifen at all points (p<0.001), which indicates enhanced anticancer potency. Blank nanoparticles exhibited poor cytotoxicity (IC<sub>50</sub> >100 μM); it confirms the carrier's biocompatibility. [56]

**Table 6:** IC<sub>50</sub> values (μM) of formulations against breast cancer cell lines

Treatment	MCF-7 (24hrs)	MCF-7 (48hrs)	MDA-MB-231 (24hrs)	MDA-MB-231 (48hrs)
Free Tamoxifen	8.6 ± 1.2	5.3 ± 0.7	15.2 ± 2.0	11.5 ± 1.6
Tamoxifen loaded NPs	4.3 ± 0.5*	2.0 ± 0.2*	7.7 ± 1.0*	4.8 ± 0.6*
Blank NPs	>100	>100	>100	>100

\*Data expressed as mean ± SD

**Evaluation of Cellular Uptake:** Evaluation of Cellular Uptake: Fluorescence microscopy and flow cytometry are used, which revealed a time-related uptake of FITC-labeled

nanoparticles in both cell lines, with peak uptake observed at 6 hrs (Table 2). MCF-7 cells demonstrated significantly higher fluorescence intensities compared to MDA-MB-231 cells across all time points (p < 0.05). [57,58]

**Table 7:** Mean Fluorescence Intensity (MFI) of FITC-labeled nanoparticles

Time(hrs.)	MCF-7	MDA-MB-231
1	244±17	186±21
2	411±33	297±30
4	688±53	445±37
6	933±70	613±46

Data expressed as mean ± SD.

**Induction of Apoptosis**

Tamoxifen-loaded NP-treated cells were compared with free tamoxifen and control for apoptosis using Annexin V-

FITC/PI staining. The results indicate an elevated apoptosis rate for Tamoxifen-loaded NPs (Table 3). After 48 h, the nanoformulation induced 1.71-fold greater apoptosis in MCF-7 and 1.7-fold in MDA-MB-231 cells relative to the free drug. [59]

**Table 8:** Apoptotic cell percentage after 48 h treatment

Treatment	MCF-7(%)	MDA-MB-231(%)
Untreated Control	2.2 ± 0.3	1.7 ± 0.2
Vehicle Control	2.1 ± 0.5	2.0 ± 0.4
Free Tamoxifen	34.6 ± 4.1	27.8 ± 3.8
Tamoxifen-Loaded NPs	59.2 ± 6.0	47.3 ± 5.2
Blank NPs	3.1 ± 0.5	2.8 ± 0.6

Data expressed as Mean ± SD

**Inhibition of Cell Migration**

Notable inhibition of cell migration was shown by the tamoxifen-loaded NPs, which was evident from the wound

healing assay, as reflected by decreased wound closure percentages when it was compared with free tamoxifen (Table 4; p < 0.001). [60]

**Table 9:** Wound closure (%) after 48hrs.

Treatment	MCF-7	MDA-MB-231
Untreated Control	78.3 ± 5.3	82.5 ± 4.9
Vehicle Control	76.8 ± 4.8	80.2 ± 5.4
Free Tamoxifen(IC <sub>20</sub> )	45.4 ± 6.0	52.8 ± 7.3

Tamoxifen-Loaded NPs(IC <sub>20</sub> )	23.2 ± 3.7	31.5 ± 4.7
---	------------	------------

Data's were expressed as Mean ±SD

## DISCUSSION

Tamoxifen-loaded agar–chitosan nanoparticles show high in vitro anticancer efficacy in comparison to free tamoxifen, which was indicated by low IC<sub>50</sub> values, high cellular uptake, higher apoptosis induction, and high anti-migratory effects. This improvement is attributed to enhanced endocytosis-mediated cellular delivery, sustained intracellular release, buffering against drug efflux, and possible synergistic effects of the polysaccharide carrier. These results provide space for further development of this nanocarrier for better breast cancer therapy. Statistical evaluation was performed using an ANOVA method followed by a Tukey post hoc test. Significance was set at  $p < 0.05$ .

## 3.4 CONCLUSION

This comprehensive study largely produced and then refined an innovative hybrid seaweed polysaccharide nanoparticle for anticancer drug delivery, stuffing significant gaps in contemporary marine biopolymer research [61]. The hybrid nanocarrier platform adds up to a transformative advancement towards sustainable, biocompatible drug delivery systems with enhanced therapeutic efficacy [62]. This study provides a solid groundwork for the practical application of seaweed polysaccharide-based nanomedicines in cancer therapy, enhancing the expanding domain of marine-derived targeted treatments. These findings not only highlight the potential of marine biopolymers for medical applications but also encourage further exploration of their unique properties. Such exploration could lead to the development of innovative solutions that address pressing medical challenges while promoting environmental sustainability. As researchers investigate the functionalities of these biopolymers, we may witness a new era of therapeutic options that harness the untapped resources of our oceans. Future research could focus on optimizing the synthesis and functionalization of these nanoparticles to maximize their effectiveness in various therapeutic contexts.

## 3.5 REFERENCE

- Algharib SA, Dayyoub E, Barkho S, et al. Effects of formulation parameters and in vitro characterization of chitosan-TPP nanoparticles. *J Mol Struct.* 2022;1258 132662.
- Kamaly N, Yameen B, Wu J, Farokhzad OC. Degradable controlled-release polymers and polymeric nanoparticles: mechanisms of controlling drug release. *Chem Rev.* 2016;116 4 2602 2663.
- Senapati S, Mahanta AK, Kumar S, Maiti P. Controlled drug delivery vehicles for cancer treatment and their performance. *Signal Transduct Target Ther.* 2018;3 7.
- Nanobiopolymers in cancer therapeutics: advancing targeted drug delivery and overcoming biological barriers. *J Mater Chem B.* 2024;12 45 11619 11661.
- Danhier F, Ansorena E, Silva JM, et al. PLGA-based nanoparticles: an overview of biomedical applications. *J Control Release.* 2012;161 2 505 522.
- Shi J, Votruba AR, Farokhzad OC, Langer R. Nanotechnology in drug delivery and tissue engineering: from discovery to applications. *Nano Lett.* 2010;10 9 3223 3230.
- Holdt SL, Kraan S. Bioactive compounds in seaweed: functional food applications and legislation. *J Appl Phycol.* 2011;23 3 543 557.
- Patel S. Therapeutic importance of sulfated polysaccharides from seaweeds: updating the recent findings. *3 Biotech.* 2012;2 3 171 185.
- Li B, Lu F, Wei X, Zhao R. Fucoidan: structure and bioactivity. *Molecules.* 2008;13 8 1671 1695.
- Rhein-Knudsen N, Ale MT, Meyer AS. Seaweed hydrocolloid production: an update on enzyme assisted extraction and modification technologies. *Mar Drugs.* 2015;13 6 3340 3359.
- Pereira L, Critchley AT. The commercial cultivation of Porphyra in Japan, Korea and China. In: Critchley AT, Ohno M, Largo DB, editors. *World Seaweed Resources.* Kanagawa: ETI BioInformatics; 2006.
- Armisen R, Galatas F. Production, properties and uses of agar. In: McHugh DJ, editor. *Production and utilization of products from commercial seaweeds.* Rome: Food and Agriculture Organization of the United Nations; 1987. p. 1 57.
- Liu M, Liu Y, Cao MJ, et al. Antibacterial activity and mechanisms of depolymerized fucoidans isolated from *Laminaria japonica*. *Carbohydr Polym.* 2017;172 294 305.
- Ale MT, Mikkelsen JD, Meyer AS. Important determinants for fucoidan bioactivity: a critical review of structure- function relations and extraction methods for fucose-containing sulfated polysaccharides from brown seaweeds. *Mar Drugs.* 2011;9 10 2106 2130.
- Necas J, Bartosikova L. Carrageenan: a review. *Vet Med.* 2013;58 4 187 205.
- Chattopadhyay K, Mateu CG, Mandal P, et al. Galactan sulfate of *Grateloupia indica*: isolation, structural features and antiviral activity. *Phytochemistry.* 2007;68 10 1428 1435.
- Montgomery DC. *Design and Analysis of Experiments.* 9th ed. New York: John Wiley & Sons; 2017.
- Box GEP, Hunter WG, Hunter JS. *Statistics for*

- Experimenters: An Introduction to Design, Data Analysis, and Model Building. New York: John Wiley & Sons; 1978.
- 2020 Aug 4;12(8):732. doi: 10.3390/pharmaceutics12080732. PMID: 32759786; PMCID: PMC7465254.
19. Luiz MT, Dutra JA, Pires ADS, et al. Design of experiments DoE) to develop and to optimize nanoformulations: A systematic review of the main factors and response variables. *Eur J Pharm Biopharm.* 2021;162:96–110.
  20. Birla D, Kumar A, Garg VK, et al. Application of quality by design in optimization of pharmaceutical nanoformulations: principle, perspectives and practices. *Curr Pharm Des.* 2025;31:12–956–977.
  21. Marine Bioactive Compounds Derived from Macroalgae as Potential Drug Delivery Vehicles. *Int J Mol Sci.* 2022;23:18–10625.
  22. Design of experiments in the optimization of nanoparticle-based drug delivery systems. *J Control Release.* 2023;358:398–419.
  23. Sanniyasi E, Gopal RK, Shaik MR, et al. In vitro anticancer potential of laminarin and fucoidan from brown seaweed *Turbinaria decurrens*. *Sci Rep.* 2023;13:14599.
  24. Wang H, Zhang R, Shen J, et al. The application of marine polysaccharides to antitumor drug delivery systems. *Carbohydr Polym.* 2024;335:122050.
  25. Smith, B.C. (2011). *Fundamentals of Fourier Transform Infrared Spectroscopy* (2nd ed.). CRC Press. <https://doi.org/10.1201/b10777>.
  26. Garg U, Chauhan S, Nagaich U, Jain N. Current advances in chitosan nanoparticles based drug delivery and targeting. *Adv Pharm Bull.* 2019;9(2):195–204.
  27. Bhumkar DR, Pokharkar VB. Studies on effect of pH on cross-linking of chitosan with sodium tripolyphosphate: A technical note. *AAPS PharmSciTech.* 2006;7(2):E138–143.
  28. A rapid protocol for synthesis of chitosan nanoparticles with controlled size and low polydispersity. *Heliyon.* 2024;10:11–e31562.
  29. Anderson MJ, Whitcomb PJ. *RSM Simplified: Optimizing Processes Using Response Surface Methods for Design of Experiments*. New York: Productivity Press; 2016.
  30. Myers RH, Montgomery DC, Anderson-Cook CM. *Response Surface Methodology: Process and Product Optimization Using Designed Experiments*. 4th ed. New York: John Wiley & Sons; 2016.
  31. Mora-Huertas CE, Fessi H, Elaissari A. Polymer-based nanocapsules for drug delivery. *Int J Pharm.* 2010;385:1–2–113–142.
  32. Weng J, Tong HHY, Chow SF. In Vitro Release Study of the Polymeric Drug Nanoparticles: Development and Validation of a Novel Method. *Pharmaceutics.* 2020 Aug 4;12(8):732. doi: 10.3390/pharmaceutics12080732. PMID: 32759786; PMCID: PMC7465254.
  33. D'Souza, S. A review of in vitro drug release test methods for nano-sized dosage forms. *Adv. Pharm.* 2014, 2014, 1–12. <https://doi.org/10.1155/2014/304757>
  34. Wallace SJ, Li J, Nation RL, Boyd BJ. Drug release from nanomedicines: Selection of appropriate encapsulation and release methodology. *Drug Deliv Transl Res.* 2012 Aug;2(4):284–92. doi: 10.1007/s13346-012-0064-4. Epub 2012 Mar 3. PMID: 23110256; PMCID: PMC3482165.
  35. Prabakaran M. Chitosan-based nanoparticles for tumor-targeted drug delivery. *Int J Biol Macromol.* 2015 Jan; 72:1313–22. doi: 10.1016/j.ijbiomac.2014.10.052. Epub 2014 Nov 3. PMID: 25450550.
  36. Zhang X, Yang X, Ji J, Liu A, Zhai G. Tumor targeting strategies for chitosan-based nanoparticles. *Colloids Surf B Biointerfaces.* 2016 Dec 1;148:460–473. doi: 10.1016/j.colsurfb.2016.09.020. Epub 2016 Sep 16. PMID: 27665379.
  37. Vermes I, Haanen C, Steffens-Nakken H, Reutelingsperger C. A novel assay for apoptosis. Flow cytometric detection of phosphatidylserine expression on early apoptotic cells using fluorescein labelled Annexin V. *J Immunol Methods.* 1995 Jul 17;184(1):39–51. doi: 10.1016/0022-1759(95)00072-i. PMID: 7622868.
  38. Brumatti G, Sheridan C, Martin SJ. Expression and purification of recombinant annexin V for the detection of membrane alterations on apoptotic cells. *Methods.* 2008 Mar;44(3):235–40. doi: 10.1016/j.jymeth.2007.11.010. PMID: 18314054.
  39. Prism 8 Statistics Guide. GraphPad Software. San Diego, California USA. Available from: [www.graphpad.com](http://www.graphpad.com)
  40. Dehariya P, Soni R, Paswan SK, Soni PK. Design of experiment based formulation optimization of chitosancoated nano-liposomes of progesterone for effective oral delivery. *J Appl Pharm Sci.* 2023; 13(06):256–270.
  41. Barabadi, H., Honary, S., Ebrahimi, P., Alizadeh, A., Naghibi, F., & Saravanan, M. (2019). Optimization of myco-synthesized silver nanoparticles by response surface methodology employing Box-Behnken design. *Inorganic and Nano-Metal Chemistry*, 49(2), 33–43. <https://doi.org/10.1080/24701556.2019.1583251>.
  42. Özer Önder, Setenay & UĞURLU, Timuçin. (2024). Application of Box-Behnken design in the optimization of chitosan nanoparticles prepared by the ionic gelation method and evaluation of dispersion stability. *Journal of Research in Pharmacy.* 28(4).

- 1057-1068. 10.29228/jrp.788.
43. Hammouda S, Haikal RR, Dawood S, El Salakawy N, Abdellatif A, Mamdouh W. Leveraging quality by design for the optimization of polycaprolactone/chitosan nanocomposites loaded with tamoxifen for breast cancer therapy. *Int J Biol Macromol.* 2025 Aug;319(Pt 1):145226. doi: 10.1016/j.ijbiomac.2025.145226.
  44. Nokhodi F, Nekoei M, Goodarzi MT. Hyaluronic acid-coated chitosan nanoparticles as targeted-carrier of tamoxifen against MCF7 and TMX-resistant MCF7 cells. *J Mater Sci Mater Med.* 2022 Feb 14;33(2):24. doi: 10.1007/s10856-022-06647-6.
  45. Fan, D., Cao, Y., Cao, M. et al. Nanomedicine in cancer therapy. *Sig Transduct Target Ther* **8**, 293 (2023). <https://doi.org/10.1038/s41392-023-01536-y>.
  46. Filip Rázga, Dominika Vnuková, Veronika Némethová, Petra Mazancová, Igor Lacík, Preparation of chitosan-TPP sub-micron particles: Critical evaluation and derived recommendations, *Carbohydrate Polymers*, Volume 151, 2016, Pages 488-499, <https://doi.org/10.1016/j.carbpol.2016.05.092>.
  47. Annika Postina, Dennis To, Katrin Zöllner, Melanie Lena Ebert, Andreas Bernkop-Schnürch, Surface charge shifting mixed micelles to overcome intestinal drug delivery barriers, *Colloids and Surfaces B: Biointerfaces*, Volume 257, 2026, 115148, <https://doi.org/10.1016/j.colsurfb.2025.115148>.
  48. Hoang NH, Le Thanh T, Sangpueak R, Treekoon J, Saengchan C, Thepbandit W, Papatthi NK, Kamkaew A, Buensanteai N. Chitosan Nanoparticles-Based Ionic Gelation Method: A Promising Candidate for Plant Disease Management. *Polymers (Basel)*. 2022 Feb 9;14(4):662. doi: 10.3390/polym14040662.
  49. Anjali Pant, Jeetendra Singh Negi, Novel controlled ionic gelation strategy for chitosan nanoparticles preparation using TPP- $\beta$ -CD inclusion complex, *European Journal of Pharmaceutical Sciences*, Volume 112, 2018, Pages 180 -185, <https://doi.org/10.1016/j.ejps.2017.11.020>.
  50. oïc Bugnicourt, Pierre Alcouffe, Catherine Ladavière, Elaboration of chitosan nanoparticles: Favorable impact of a mild thermal treatment to obtain finely divided, spherical, and colloidally stable objects, *Colloids and Surfaces A: Physicochemical and Engineering Aspects*, Volume 457, 2014, Pages 476-486.
  51. Yang Xing, Weiguang Shen, Chuan Sun, Ruyi Wang, Bo Fan, Guixian Liang, Genistein-Chitosan Derivative Nanoparticles for Targeting and Enhancing the Anti-Breast Cancer Effect of Tamoxifen In Vitro, *Journal of Pharmaceutical Sciences*, Volume 113, Issue 8, 2024, Pages 2575-2583. <https://doi.org/10.1016/j.xphs.2024.05.023>.
  52. Barbieri, Stefano Sonvico, Fabio Como, Caterina Colombo, Gaia Zani, Franca Buttini, Francesca Bettini, Ruggero Rossi, Alessandra Colombo, Lecithin/chitosan controlled release nanopreparations of tamoxifen citrate: Loading, enzyme-trigger release and cell uptake. *Journal of Controlled Release* 167(3):p 276-283, May 2013. | DOI: 10.1016/j.jconrel.2013.02.009.
  53. Yedi Herdiana, Nasrul Wathoni, Shaharum Shamsuddin, Muchtaridi Muchtaridi. Scale-up polymeric-based nanoparticles drug delivery systems: Development and challenges. *OpenNano*, Volume 7, July–August 2022, 100048. <https://doi.org/10.1016/j.onano.2022.100048>
  54. Vivek R, Nipun Babu V, Thangam R, Subramanian KS, Kannan S. pH-responsive drug delivery of chitosan nanoparticles as Tamoxifen carriers for effective anti-tumor activity in breast cancer cells. *Colloids Surf B Biointerfaces*. 2013 Nov 1;111:117-23. doi: 10.1016/j.colsurfb.2013.05.018. Epub 2013 May 22.
  55. Amina Akhlaq, Muhammad Ashraf, Muhammad Ovais Omer, Imran Altaf. Carvacrol-Fabricated Chitosan Nanoparticle Synergistic Potential with Topoisomerase Inhibitors on Breast and Cervical Cancer Cells. *ACS Omega* 2023 8 (35), 31826-31838 DOI: 10.1021/acsomega.3c03337
  56. Day CM, Hickey SM, Song Y, Plush SE, Garg S. Novel Tamoxifen Nanoformulations for Improving Breast Cancer Treatment: Old Wine in New Bottles. *Molecules*. 2020 Mar 5;25(5):1182. doi: 10.3390/molecules25051182.
  57. Hu CS, Chiang CH, Hong PD, Yeh MK. Influence of charge on FITC-BSA-loaded chondroitin sulfate-chitosan nanoparticles upon cell uptake in human Caco-2 cell monolayers. *Int J Nanomedicine*. 2012;7:4861-72. doi: 10.2147/IJN.S34770. Epub 2012 Aug 10.
  58. Ge Y, Zhang Y, He S, Nie F, Teng G, Gu N. Fluorescence Modified Chitosan-Coated Magnetic Nanoparticles for High-Efficient Cellular Imaging. *Nanoscale Res Lett*. 2009 Jan 16;4(4):287-295. doi: 10.1007/s11671-008-9239-9.
  59. Fatemizadeh M, Tafvizi F, Shamsi F, Amiri S, Farajzadeh A, Akbarzadeh I. Apoptosis Induction, Cell Cycle Arrest and Anti-Cancer Potential of Tamoxifen-Curcumin Loaded Niosomes Against MCF-7 Cancer Cells. *Iran J Pathol*. 2022 Spring;17(2):183-190. doi: 10.30699/IJP.2022.124340.2356. Epub 2022 Feb 28.
  60. Moin A, Wani SUD, Osmani RA, Abu Lila AS, Khafagy ES, Arab HH, Gangadharappa HV, Allam AN. Formulation, characterization, and cellular toxicity assessment of tamoxifen-loaded silk fibroin nanoparticles in breast cancer. *Drug Deliv*. 2021

- Dec;28(1):1626-1636.  
10.1080/10717544.2021.1958106.
61. Venkatesan J, Anil S, Kim SK, Shim MS. Seaweed Polysaccharide-Based Nanoparticles: Preparation and Applications for Drug Delivery. *Polymers (Basel)*. 2016 Jan 26;8(2):30. doi: 10.3390/polym8020030. PMID: 30979124;
- doi: 62. Erebor JO, Agboluaje EO, Perkins AM, Krishnakumar M, Ngwuluka N. Targeted Hybrid Nanocarriers as Co-Delivery Systems for Enhanced Cancer Therapy. *Adv Pharm Bull*. 2024 Oct;14(3):558-573. doi: 10.34172/apb.2024.046. Epub 2024 May 15.